

Photoemission yield under two-quantum excitation in Si

M. Bensoussan, J. M. Moison, B. Stoesz, and C. Sébenne*
*Centre National d'Etudes des Télécommunications, Division RPC, † 196 rue de Paris,
 92220 Bagnex, France*
 (Received 19 June 1980)

It is shown for the first time that under pulsed laser excitation, photoemission from cleaned (7×7) Si (111) surfaces occurs at photon energies (3.7 to 2.3 eV) below the work function ($\phi = 4.6$ eV). We demonstrate its two-quantum origin by: (i) establishing the characteristic flux law, i.e., electron flux proportional to the square of photon flux, over six orders of magnitude; (ii) showing that the two-quantum yield falls very rapidly when photon energy decreases, no photoemission being observed below $\frac{1}{2}\phi$.

I. INTRODUCTION

A number of experiments on multiquantum photoemission from solids, under very intense laser irradiation, have been reported in the past few years.¹ The most salient features of these effects are that the laser photon energy lies below the work function of the target material and that the photoelectron flux J_e ($\text{cm}^{-2} \text{s}^{-1}$) is proportional to J_{ph}^n , where J_{ph} is the laser photon flux ($\text{cm}^{-2} \text{s}^{-1}$) and n the order of the effect. Most of the experiments have been carried out on metals² and only a few of them on semiconductors, mainly photocathodes coatings such as Cs_3Sb (Ref. 3) and K_3Sb .⁴

The experimental observation of multiquantum photoemission presents a number of difficulties. First, because of its small quantum yield, it requires very powerful pulsed laser sources to be observed; therefore, interferences with thermal emission, owing to the heating of the sample,⁵ have to be strictly avoided. This can be achieved by taking advantage of the recent progresses of weak photocurrent detection methods and by a proper choice of the pulse duration and of the focusing conditions. Moreover, the analysis of the effect, because of its nonlinearity, demands a careful determination of the illumination conditions. Such determination had not been systematically performed up to now.

In this paper we wish to present the first observation of true two-quantum photoemission from well-defined Si surfaces, with laser photon energies below the first-order threshold⁶ ($\phi = 4.6$ eV). This is unambiguously demonstrated in two steps. First it is shown that the observed photocurrent indeed results from a double-quantum emission and not from a thermal effect, by establishing that the electron and the photon fluxes are related by

$$J_e = \beta J_{\text{ph}}^2, \quad (1)$$

where, for each photon energy, β is a constant independent of the geometrical parameters. Then β is shown to exhibit a two-quantum photoemission threshold around one-half the value of the first-order one.

II. EXPERIMENTAL

The experimental setup is described in Fig. 1. The strong light intensities required are provided either by a nitrogen laser or by a dye laser pumped by the former. The pulse time dependences are measured with a fast photodiode and a sampling oscilloscope; their half-widths are, respectively, 3.5 and 1.7 ns. The laser beam impinges on the sample at near normal incidence and is specularly reflected out of the UHV

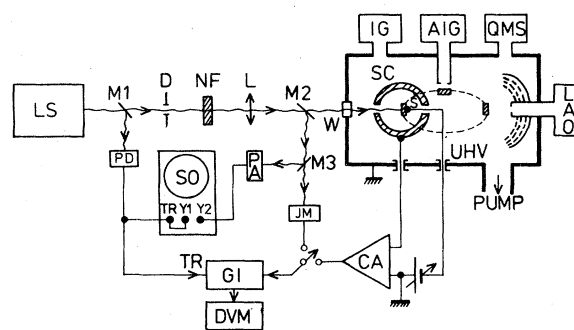


FIG. 1. Experimental setup. AIG: argon ion gun; CA: charge amplifier; D: diaphragm; DVM: digital voltmeter; GI: gated integrator; IG: ionization gauge; JM: joulemeter; L: lens; LAO: LEED/AUGER optics; LS: laser source; M1: semitransparent mirror; M2, M3: removable mirrors; NF: neutral filter; PD: fast photodiode; QMS: quadrupole mass spectrometer; S: sample; SC: spherical collector; SO: sampling oscilloscope; TR: trigger pulse.

chamber along the reverse optical path. Since the effect to be studied is very sensitive to the light energy distribution on the sample, we have characterized our laser beams very carefully. The beam total energy W on the sample is measured by a calibrated pyroelectric detector. At maximum, it reaches 10^{-4} J and can be varied by calibrated neutral filters. A small fraction of the beam is directed toward a linear array of 128 photodiode-capacitor cells ($25 \times 25 \mu\text{m}$ each) located in a plane optically equivalent to that of the sample. By translating mechanically the photodiode array in its plane we obtain a map of the energy distribution on the sample, integrated over the $(25 \mu\text{m})^2$ elementary diode area and expressed by a $(\Delta W/\Delta S)_{ij}$ contour matrix. An example of such a map is given in Fig. 2. The energy distribution can be varied by using diaphragms and by changing the focusing conditions.

The sample is a (111) oriented n -type silicon wafer with $n = 10^{19} \text{ cm}^{-3}$. It has been chemically cleaned, then prepared under ultrahigh vacuum by ion bombardment and annealing until a clean, (7×7) recon-

structed surface is obtained. Surface characterization is obtained from low-energy electron diffraction and Auger spectroscopy measurements. The pressure in the vacuum system during all experiments is about 1×10^{-10} Torr.

Photoelectrons are collected by a near-ground spherical collector centered on the sample, which is brought to a negative potential. The value of this potential is taken high enough to make space-charge effects negligible; such effects are actually observed at low voltages (a few volts) under strong laser illumination. The collector is connected to a solid-state charge amplifier coupled to a gated integrator, the output of which is proportional to the mean value of the photoelectric charge per laser pulse averaged over a few hundred pulses. The noise limit is about 5×10^{-17} C, i.e., 300 electrons.

III. RESULTS AND DISCUSSION

During the experiments we have measured systematically four quantities: (i) the laser total energy on the target W , (ii) the pulse temporal shape $\partial W/\partial t$, (iii) the laser pulse energy distribution on the target $(\Delta W/\Delta S)_{ij}$, and (iv) the photoelectric charge per pulse Q . $\partial W/\partial t$ is a characteristic of our lasers and cannot be tuned, but the effect of the variations of both W and $(\Delta W/\Delta S)_{ij}$ on Q were investigated. The experimentally measured quantities are related to the fluxes by

$$W = h\nu \iint J_{\text{ph}} ds dt, \quad Q = e \iint J_e ds dt. \quad (2)$$

Let us introduce the dimensionless spatial and temporal pulse profiles σ and θ such that the photon flux can be written as a function of its peak value J_{ph}^M as

$$J_{\text{ph}} = J_{\text{ph}}^M \sigma(x, y) \theta(t). \quad (3)$$

If the relation (1) holds, then the peak electron flux J_e^M and the peak photon flux are related by

$$\begin{aligned} J_e^M &= Q/eS_2T_2 = \beta(J_{\text{ph}}^M)^2 \\ &= \beta(W/h\nu S_1 T_1)^2, \end{aligned} \quad (4)$$

where T_1 , T_2 , S_1 , and S_2 are integrals which depend only on $\partial W/\partial t$ and $\partial W/\partial S$ and are expressed in Ref. 7. As long as the spatial extension of the beam is wider than the instrument resolution, S_1 and S_2 can be calculated numerically from the photodiode array energy distribution mapping (Fig. 2).

When the energy distribution over the target is uniform, $\partial W/\partial S = W/S$ and Eq. (4) takes a simpler form

$$Q = [eT_2/(h\nu T_1)^2] \beta (W^2/S). \quad (5)$$

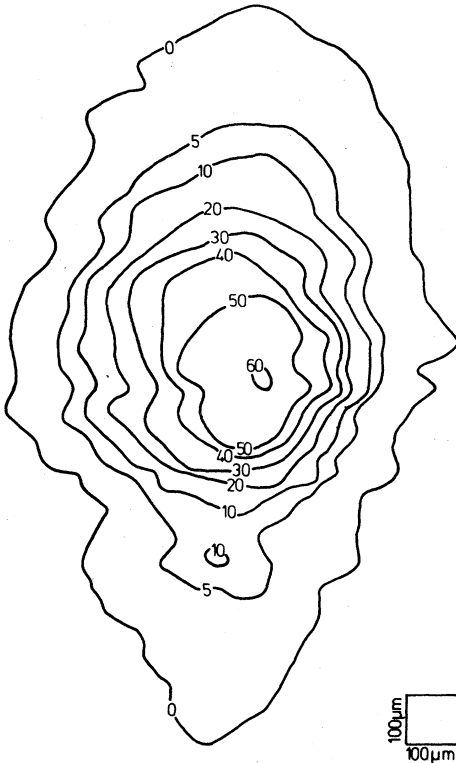


FIG. 2. Energy distribution map leading through numerical integration to $S_1 = 0.19 \text{ mm}^2$, $S_2 = 0.11 \text{ mm}^2$, and to a value of β in agreement with the one obtained under uniform-beam conditions. It may be noted that a simpler full-width-at-half-maximum-type determination would lead to $S_1 = 0.20 \text{ mm}^2$ and $S_2 = 0.10 \text{ mm}^2$, i.e., a 20% error on β . (See text for definition of S_1 and S_2 .)

This condition can be satisfied in a certain range of focusing by use of diaphragm and by moving the lens focus well off the sample.

The first set of data was obtained with the N_2 laser output, and was aimed to establish that either Eq. (5) or (4) indeed holds in our configuration. In the uniform energy distribution regime, which was experimentally found to correspond to $S \geq 1 \text{ mm}^2$, we have verified the validity of Eq. (5) by varying independently W and S . Typical data are shown in Figs. 3(a)

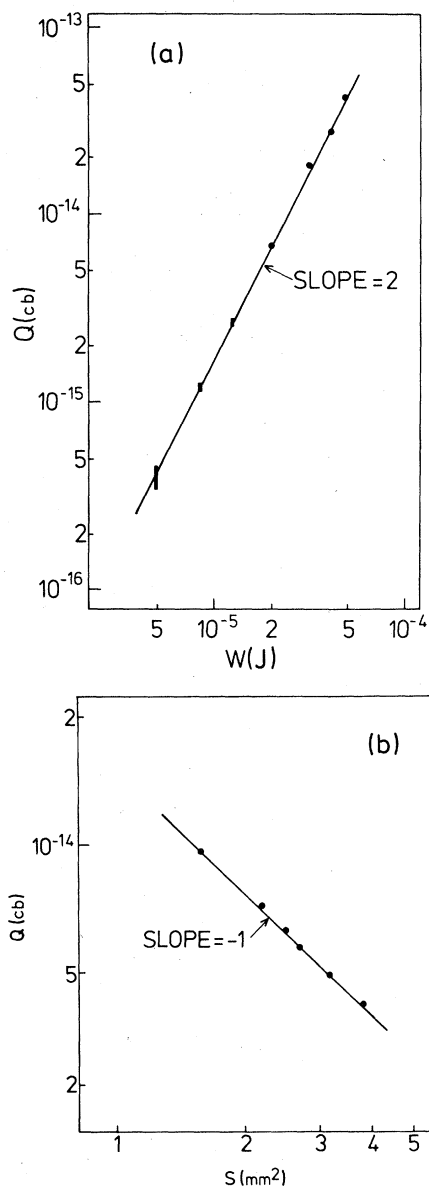


FIG. 3. Log-log plots of the charge per pulse Q , photoemitted by Si (111), vs (a) beam energy W with a constant impact area of 2 mm^2 , (b) impact area S with a constant beam energy of $2 \times 10^{-5} \text{ J}$. The photon energy is 3.68 eV .

and 3(b), where $\log(Q)$ is plotted versus $\log(W)$ at constant S and $\log(S)$ at constant W , respectively, evidencing the $+2$ and -1 expected slopes. For a tighter focusing ($S < 1 \text{ mm}^2$), the energy distribution uniformity cannot be held and the numerical determination of S_1 and S_2 becomes necessary. The electron and photon fluxes are then computed according to Eq. (4). The data corresponding to the tight focusing and the uniform distribution regime are collected in the single $\log(J_e)$ vs $\log(J_{ph})$ diagram shown in Fig. 4. An excellent fit over six orders of magnitude is found, for irradiation spot areas ranging from 0.04 mm^2 (nearly Gaussian beam) to 4 mm^2 (homogeneous energy distribution). This result establishes clearly the spatial independence of β down to the $100\text{-}\mu\text{m}$ scale. Since no edge effect is observed, any mean free path or diffusion length involved in the two-quantum process must be very short compared to that length at the present photon energy. The best value deduced from our measurement is $\beta = (10.5 \pm 1.5) \times 10^{-34} \text{ cm}^2 \text{ s}$ at $h\nu = 3.68 \text{ eV}$.

The double-quantum origin of the observed photocurrent being established, we have in a second set of experiments used the dye laser to extend to lower photon energies the measurement of β . For three additional energies we have checked the indepen-

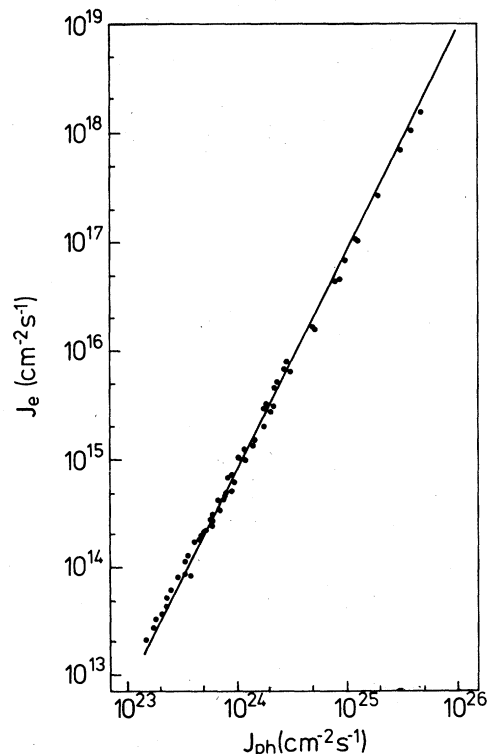


FIG. 4. Log-log plot of the photoelectron flux J_e vs photon flux J_{ph} for $h\nu = 3.68 \text{ eV}$.

TABLE I. Values of β for different photon energies.

$h\nu$ (eV)	3.68	3.02	2.53	2.30
β (10^{-37} cm ² s)	10 500	350	7	< 1 ^a

^a1 is our experimental noise limit.

dence of β on the spot size in a way analogous to that described above and determined its magnitude accordingly. Our results are reported in Table I; β decreases by four orders of magnitude when the photon energy varies from $h\nu = 3.68$ to 2.3 eV. At this energy and below, no two-quantum photoemission could be observed. This double-quantum photoemission threshold behavior has to be referred to the work function and ionization energy values (actually, it should be compared to one-half their values) of a clean (7×7) Si (111) surface, which are, respectively,⁸ $\phi = 4.6 \pm 0.1$ eV and $I = 5.4 \pm 0.1$ eV. From Table I, it is clear that the double-quantum photoemission yield is consistent with the work function value. This supports the assumption that the process is a combination of two elementary excitations. Since the bulk states contribution should appear only at photon energies higher than 2.7 eV in the case of heavily doped *n*-type samples, photoemission observed at $h\nu = 2.53$ eV must originate from intrinsic gap surface states, which are known to exist in that

energy range from linear photoemission measurements.⁸ This threshold behavior also shows that the greatest care must be taken when giving a value of β for a single-photon energy, particularly if one means to account for it by some theory. Indeed, our results cover approximately the whole range of β values reported in the literature for various materials and photon energies (see Table II). The very disparity of these values makes any discussion hazardous especially if one considers the variety of experimental conditions.

A few remarks can be made about the elementary processes accountable for the observed two-quantum photoemission. Among all the processes which can be put forward to interpret the results probably the most important are the following ones:

(a) A two-photon absorption where the electron is first pumped to a real or a virtual excited state and subsequently absorbs a second photon. The electron then reaches a final state above the vacuum level. This kind of process was observed by nonlinear ab-

TABLE II. Materials, work functions, laser photon energies, and two-photon parameters of the literature.

Materials	ϕ (eV)	$h\nu$ (eV)	β (cm ² s)
Ta ^a	4.13	2.33	8.7×10^{-36}
Mo ^a	4.41	2.33	5.2×10^{-37}
W ^a	4.49	2.33	4.4×10^{-37}
Na ^b	2.3	1.96	5.5×10^{-33}
		1.48	2.8×10^{-34}
Au ^b	4.8	3.57	4.9×10^{-33}
Stainless steel ^b			
	5.0	3.57	8.6×10^{-33}
CsI ^b	6.1	3.57	6.5×10^{-31}
KI ^b	7.0	3.57	6.1×10^{-31}
Cs ₃ Sb ^b	1.8–2.0	1.17	1.31×10^{-29}
			4.6×10^{-30}
			9.2×10^{-31}
K ₃ Sb ^b	2.2–2.9	1.78	2.0×10^{-31}

^aReference 2.

^bReference 1.

sorption in Si (Ref. 9) but unfortunately not at the same wavelength as in the present work.

(b) A nonradiative Auger process which is known to be one of the dominant recombination process in Si at high carrier photoinjection.¹⁰

However it is not possible at the present time to identify unambiguously the microscopic origin of the observed photocurrent; clearly, more investigations,

both theoretical and experimental, are needed to settle down this point.

ACKNOWLEDGMENT

The authors thank D. S. Chemla for fruitful discussions and comments on the manuscript.

*Permanent address: Laboratoire de Physique des Solides, associé au CNRS Université P. et M. Curie Paris, France.

†Laboratoire associé au CNRS (LA 250).

¹P. P. Barashev, *Phys. Status Solidi (a)* **9**, 9 (1972).

²J. H. Bechtel, W. Lee Smith, and N. Bloembergen, *Phys. Rev. B* **15**, 4557 (1977); R. Yen, P. Liu, M. Dagenais, and N. Bloembergen, *Opt. Commun.* **31**, 334 (1979).

³H. Sonnenberg, H. Heffner, and W. Spicer, *Appl. Phys. Lett.* **5**, 95 (1964).

⁴S. Imamura, F. Shiga, K. Kinoshita, and T. Suzuki, *Phys. Rev.* **166**, 322 (1968).

⁵J. F. Ready, *Effects of High Power Laser Radiation* (Academic, New York, 1971).

⁶C. Sebenne, D. Bolmont, G. Guichar, and M. Balkanski, *Phys. Rev. B* **12**, 3280 (1975).

⁷As a function of $\sigma(x,y)$ and $\theta(t)$ one has

$$T_l = \int [\theta(t)]^l dt = \int \frac{(\partial W / \partial t)^l dt}{[(\partial W / \partial t)^M]^l}$$

$$S_l = \int [\sigma(x,y)]^l dt = \int \frac{(\partial W / \partial S)^l ds}{[(\partial W / \partial S)^M]^l}$$

where the superscript M indicates peak values.

⁸G. M. Guichar, C. A. Sebenne, G. A. Garry, and M. Balkanski, *Surf. Sci.* **58**, 374 (1976).

⁹J. F. Reintjes and J. C. McGroddy, *Phys. Rev. Lett.* **30**, 901 (1973).

¹⁰K. G. Svantesson and N. G. Nilsson, *Solid State Electron.* **21**, 1603 (1978).